Treatment planning for molecular targeted radionuclide therapy

Christine L. Hartmann Siantar,[1] Kai Vetter,[1] Gerald L. DeNardo[2] and Sally J. DeNardo[2]

Running Title: Treatment Planning

[1]Glenn T. Seaborg Institute, Lawrence Livermore National Laboratory, Livermore, California

[2]Radiodiagnosis and Therapy, Division of Hematology/Oncology, University of California Davis Medical Center, Sacramento, California

Key words: radionuclide, dosimetry, therapy, radiotherapy, cancer, radiation detection

Corresponding Author:

Christine L. Hartmann Siantar, Ph.D.
Glenn T. Seaborg Institute
L-231
Lawrence Livermore National Laboratory
Livermore, CA 94550
Phone: 925-422-4619
Fax: 925-423-9719
E-mail: chs@llnl.gov

Treatment planning for molecular targeted radionuclide therapy

Christine Hartmann Siantar, Kai Vetter, Gerald DeNardo, and Sally DeNardo

Summation

Molecular targeted radionuclide therapy promises to expand the usefulness of radiation to successfully treat widespread cancer. The unique properties of radioactive tags make it possible to plan treatments by predicting the radiation absorbed dose to both tumors and normal organs, using a pre-treatment test dose of radiopharmaceutical. This requires a combination of quantitative, high-resolution, radiation-detection hardware and computerized dose-estimation software, and would ideally include biological dose-response data in order to translate radiation absorbed dose into biological effects. Data derived from conventional (external beam) radiation therapy suggests that accurate assessment of the radiation absorbed dose in dose-limiting normal organs could substantially improve the observed clinical response for current agents used in a myeloablative regimen, enabling higher levels of tumor control at lower tumor-to-normal tissue therapeutic indices. Treatment planning based on current radiation detection and simulations technology is sufficient to impact on clinical response. The incorporation of new imaging methods, combined with patient-specific radiation transport simulations, promises to provide unprecedented levels of resolution and quantitative accuracy, which are likely to increase the impact of treatment planning in targeted radionuclide therapy.

Acknowledgements

The authors would like to thank Dr. Lawrence Williams, Dr. Ignacio Azinovic and Dr. Mortimer Mendelson for their helpful input. This research was supported by grants from the U.S. Department of Energy Office of Biological and Environmental Research and the National Cancer Institute). This work was performed under the auspices of the U.S. Department of Energy by the Lawrence Livermore National Laboratory under Contract W-7405-ENG-48.

Introduction

Over the last decade, an increasing number of laboratory and clinical studies have pointed to the dramatic potential of using molecular targeting agents, tagged with radionuclides, to treat metastatic cancer. The resulting targeted radionuclide therapy uses cancer-seeking molecules to biologically deliver cytotoxic ionizing radiation to cancer throughout the body. This approach extends the therapeutic role of ionizing radiation, which is already used to control localized disease for about half of all cancer patients.[1] The most well-established agents are monoclonal antibodies, while many promising new types of molecular constructs are actively being developed. Response rates as high as 50-80%, for monoclonal antibodies targeting non-Hodgkin's lymphoma point to the promise of this novel form of cancer therapy.[2]

One of the key challenges in targeted radionuclide therapy is to optimize drug administration and determine in advance which patients will most benefit. Targeted radionuclide therapy has a unique feature that can be exploited for this purpose: the radioactive atoms generally carried by the targeting agent often emit both short-range electrons, which deliver the cytotoxic radiation absorbed dose, and long-range gamma rays (energetic photons), which can be

imaged outside the body. The result is that a diagnostic test dose of radiolabeled drug, combined with 2- and 3-D radiation imaging, can be used to quantify the time-dependent location of the drug/radionuclide, calculate the corresponding radiation dose to tumor(s) and normal organs, and ultimately estimate both tumor control and normal tissue complications before the patient is treated with a therapeutic drug dose.

This paper describes the goal of treatment planning, why it is important, and how it is likely to be improved in the next decade. Analysis based on tumor and normal tissue dose response data from conventional radiation therapy, suggests that in a myeloablative regimen, at current therapeutic indices, uncertainty in the assessment of radiation absorbed dose in radiation-sensitive normal organs can make a substantial impact on the uncomplicated tumor control probability. For currently-observed therapeutic indices, changing the basis of treatment prescription from administered mCi to accurate absorbed dose in the treatment-limiting organ is equivalent to increasing the therapeutic index (relative amount of drug targeting) by as much as 50-100%.

Treatment Planning

The goal of treatment planning is to provide information that enables the physician to optimize the prescription of a targeted radionuclide and estimate its potential benefit to the patient. This requires a standard *metric* for quantifying clinical effects in terms of amount of radiopharmaceutical delivered, *clinical data* to relate the metric to patient response, and a technology-based *treatment planning system* that reliably predicts the metric (and ultimately patient response) from pre-treatment data.

Metric: absorbed radiation dose

The first challenge is to determine the best metric for quantifying the administration and effects of targeted radiopharmaceuticals. In most patient trials to date, targeted radionuclide therapy has been quantified in terms of drug (radioisotope activity) administered per unit mass or surface area of the patient (mCi/kg or mCi/m^2), following the chemotherapy paradigm. This contrasts with conventional radiation therapy, whose delivery is quantified as a distribution of radiation absorbed dose, the amount of radiation energy absorbed per unit mass of tissue (Gy, where 1 Gy=1 J/kg).

If the primary therapeutic mechanism of targeted radionuclide therapy is radiation damage, it makes sense to rely on the metric of radiation absorbed dose to guide its quantification and prescription. In reality, the physical deposition of radiation energy, quantified as absorbed dose, is actually only one of several factors that affect tissue response to radiation: radiosensitizers, the time-dependence of dose delivery, the energy and type of radiation dose-delivery particles, and other factors can alter the radiation's biological effects. Nevertheless, the value of radiation absorbed dose as a primary radiation-delivery metric has been well established in radiation biology and radiation oncology over the last several decades.[3-9]

Treatment planning links the amount of administered radionuclide to radiation absorbed dose in the patient. Thus it enables prescription of targeted radionuclide based on anticipated patient response, in terms of tumor control and normal tissue complications.

Clinical data

The next challenge is to relate the metric, radiation absorbed dose, to *clinical data* describing patient response: tumor control and radiation damage to normal organs. At current targeting levels, radiation toxicity to normal organs is a key part of the effectiveness equation. Because of the modest amount of clinical data for targeted radionuclide therapy,[10] we use more established and readily-available clinical response data from conventional radiation therapy to provide examples of radiation toxicity. The real challenge is to develop and assess these concepts with actual targeted radionuclide therapy data. Accurate, patient-specific dose estimates, as described below, should greatly enhance the reliability of this process.

Also, for many trials conducted up to this point, the most sensitive (dose-limiting) organ is bone marrow. So far, radiation dose to bone marrow has not proven to be a completely reliable predictor of bone marrow toxicity, probably due to a host of significant biological and dosimetric uncertainties particular to this organ, including complicated geometries whose critical features span microscopic to macroscopic dimensions, large fluctuations in functional reserve due to previous cancer therapy, and disease in the bone marrow itself.[11] To simplify this discussion, we assess treatment planning needs and objectives for myeloablative therapy. Therefore, bone marrow dosimetry can be avoided and the critical, radiation-sensitive organs are likely to be the lungs, kidneys, and liver.

Treatment planning system

Finally, prescribing targeted radionuclide therapy based on radiation absorbed dose requires a system of technology for accurately detecting radioisotope concentration in the body and predicting radiation absorbed dose in tumor(s) and normal organs. This system must be simple and inexpensive enough to be used on every patient, yet accurate enough to measurably impact patient outcome.

Prescription according to radiation absorbed dose is necessarily indirect: first, the radiation absorbed dose is estimated; next, radiation absorbed dose is used to determine the activity to be administered. This follows a paradigm developed in conventional radiation therapy.[1]

In targeted radionuclide therapy, the targeting agent optimizes the tumor dose through biological delivery. The role of the treatment planner is to quantify how well the cancer has been targeted and guide decisions on how much radionuclide (mCi) to administer. To accomplish this, the treatment planning system must quantify the relationship between administered activity and absorbed radiation dose in the dose-limiting normal organs and estimate the ratio of absorbed dose in the tumor(s) and normal organs.

The ideal treatment planning system would

- Determine the time-dependent radiation (activity) distribution in the patient, using images obtained with a diagnostic test-dose of targeted radioisotope drug.
- Estimate the distribution of radiation absorbed dose in tumor(s) and normal organs per administered radiopharmaceutical activity
- Provide information that guides the clinician on whether or not to treat the patient and how much activity to administer

- Allow retrospective analysis of doses (and dose rates) delivered during treatment

The essential input for this type of system is a series of quantitative 2- and 3-dimensional activity distributions in the patient, combined with a 3-dimensional map of the patient's anatomy. The basic output of a treatment planning system consists of time-integrated absorbed dose distributions in the patient's tumor(s) and sensitive normal organs. As more reliable biological-response data for targeted radionuclide therapy becomes available, this information could be folded into the output, to allow the clinician to prescribe the radionuclide dose that maximizes the patient response.

Why Treatment Planning Is Important

Treatment planning is important because it provides a mechanism for optimizing the treatment for each individual patient. It can also be expensive to implement in clinical trials. Using radiation response information obtained from conventional radiation therapy, we can estimate the relative importance of accurate treatment planning compared to other advances such as improved drug targeting.

Radiation Response Parameters

Over the course of several decades, animal and human studies aimed toward improving conventional radiation therapy have shown that tumor control probability (TCP) and normal tissue complication probability (NTCP) increase with radiation absorbed dose, following a sigmoidal shape. Dose response has been fit by a variety of models, all of which result in the same general S shape, and are clinically indistinguishable. For the rest of this discussion we use the logistic function[12, 13]:

$$P(D) = 1/(1+(D_{50}/D)^{k})$$

Where P is the probability of a clinical effect, D is radiation absorbed dose, D_{50} is the radiation absorbed dose which leads to 50% cure/complication probability and k is a parameter describing the slope of the dose-response curve.

Figure 1 shows examples of dose response for tumor (A) and normal tissue (B) observed in conventional radiation therapy.[8, 14, 15] The carcinoma tumor control probability curve was fit to the dose-response data reported for carcinoma of the nasopharynx for T1-2 and T3-4 tumors,[14] while the lymphoma dose-response curve was fit to dose-response probabilities reported for Hodgkin's lymphoma.[16] The representative lymphoma and carcinoma tumor-control curves are shown in order to demonstrate the impact therapeutic indices for relatively more- and less-radiosensitive cancers.

For molecular targeted radiation therapy following a myeloablative strategy, the most sensitive critical organs are the lung, liver, and kidneys. The normal tissue complication probability parameters shown in Figure 1 were chosen to fit the full-organ tolerance doses for 5% and 50% complication probabilities, summarized by Burman et al.[15] Complication (tolerance) endpoints are clinical pneumonitis, liver failure, and nephritis, respectively.

To plot tumor control and normal tissue complication probability on the same graph, one must account for the fact that, for a given treatment, more drug (and radiation absorbed dose) is targeted to the tumor than to normal tissue. We account for drug targeting by replacing tumor control probability by the *effective* tumor control probability (eTCP):

$$eTCP(D_{NT}) = TCP(D_T / \text{therapeutic index})$$

where D_{NT} and D_T are the radiation absorbed dose in the normal tissue and tumor, respectively, and the therapeutic index is defined as

$$\text{therapeutic index} = \frac{\text{(average radiation absorbed dose in the tumor)}}{\text{(average radiation absorbed dose in a normal organ)}}$$

for an administered unit of radioactivity. Quantifying tumor control as eTCP allows tumor-control and normal-tissue-complication probabilities to be directly compared for patients with a given therapeutic index. With tumor control and normal tissue complications on the same plot, we can now calculate the uncomplicated tumor control probability (UTCP), or the probability of tumor control minus the probability of significant normal tissue complication.

$$UTCP(D_{NT}) = eTCP(D_{NT}) - NTCP(D_{NT})$$

UTCP is similar to the uncomplicated tumor ablation concept described by Mendelsohn.[17] Because it quantifies the likelihood of treatment success in the context of both tumor control and normal tissue complications, UTCP provides a more realistic overall metric than either tumor control or normal tissue complication probability alone.

Figure 2 shows NTCP, eTCP, and the resulting UTCP, for the kidney (clinical nephritis) and carcinoma data described in Figure 1, assuming a therapeutic index of 3. The UTCP follows the effective tumor control (eTCP) curve until the probability of normal tissue complications (NTCP) begins to rise. The maximum uncomplicated tumor control probability occurs at the dose at which the slopes of the eTCP and NTCP curve are the same.

It should be made clear that this analysis, using current data, provides only rough guidance on expected trends, because we have approximated dose-response (TCP and NTCP) curves for targeted radionuclide therapy with data derived from conventional radiation therapy: these values may not translate directly, due to dose rate and other effects. Some evidence of the consistency of targeted radionuclide and conventional radiation therapy is provided by the observation by Press et al.[18] of a maximum tolerated dose for lung at 27 Gy, somewhat higher, but not completely inconsistent with the $TD_{5/5}$ dose (5% probability of complications within five years) of 17.5 Gy, tabulated by Emami et al.[8]

In an effort to estimate patient response for practically-attainable treatments, we estimate a therapeutic index range from the experience described for a group of 70 patients with non-Hodgkin's lymphoma, enrolled in a trial to assess the relative merits of ^{67}Cu-2IT-BAT-Lym-1, ^{131}I-Lym-1 and ^{90}Y=2IT-BAD-Lym-1.[19]. In this study, therapeutic index values ranging from 1-9 for lung, 1.5-9 for kidney, and 1-6 for liver were observed. This observation is generally consistent with the therapeutic indices of 1.8 ± 0.2, 3.4 ± 0.3, 3.0 ± 0.3 for lungs, kidneys, and liver, measured by Press et al.[18] for 19 B-cell lymphoma patients with favorable biodistributions, who were treated with ^{131}I-labeled anti-CD20 and anti-CD37 antibodies. For advanced carcinoma of the breast, DeNardo et al.[20] observed radiation absorbed doses of 2.5 ± 1.5, 2 ± 1.5, and 13.5 ± 13.2 cGy/mCi in lung, liver and tumors. This would have resulted in average therapeutic ratios of about 5 for lung and 7 for liver.

Figure 3 plots the maximum UTCP as a function of therapeutic index for lung, kidney, and liver. This superposition suggests that patient tumors displaying the therapeutic indices superposed here would have a reasonably high potential for uncomplicated tumor control for lymphoma. However, patient tumors with therapeutic indices of about 4.5 or greater would be required to observe a similar potential for carcinoma. Figure 3 plots only the maximum possible

uncomplicated tumor control, in a uniform-therapeutic index system. Actual tumor control for a specific patient would depend on the amount of radioactive drug administered. For a tumor-lung therapeutic index measured at 1.8, the maximum UTCP of 86% for lymphoma – lung plotted in Figure 3 in generally consistent with the 84% complete response rate (tumor control for measurable tumors) observed by Press et al.[18].

Impact of Absorbed Radiation Dose Heterogeneity and Uncertainty

At first glance, Figure 3 suggests that lymphoma and carcinoma should be well on their way to being cured with therapeutic indices available now. However, heterogeneity in absorbed radiation dose in the tumor(s) and uncertainty in absorbed dose in normal tissues substantially cloud this optimistic picture. Heterogeneity in absorbed radiation dose to the cancer is primarily driven by variations in radionuclide concentration (targeting) and escaping charged particles in small masses. Technological advances in imaging and radiation simulations can only aspire to better quantify tumor dose heterogeneity and predict its impact on uncomplicated tumor control, leading to better patient selection. However, imaging and simulations can make a substantial impact on reducing the uncertainty in estimates of absorbed radiation dose to the dose-limiting normal organs. As we show in this section, this could substantially improve the uncomplicated tumor control currently observed in patient trials.

A key factor in absorbed dose variation in a patient with metastatic cancer is charged particle escape. Absorbed radiation dose is measured in tumors that are large enough to accumulate a quantifiable amount of radioactivity: diameters greater than 1 cm. In reality, a patient with metastatic cancer would be expected to have cancer sites ranging in size from a few cells to large tumors. In order to cure the patient, cancer cells must be eradicated at the microscopic level. Nahum and others have shown that as tumor size decreases, the dose delivered by the radionuclide decreases as well, because electrons carry their energy outside the cancer boundaries.[21-23] This effect is offset by the theoretically greater radiosensitivity of smaller tumors. In addition, uptake of radiometals goes inversely to tumor mass, giving the smallest tumors a greater amount of radioactivity, and hence a higher radiation absorbed dose. For a neuroblastoma model, Nahum showed that charged particle escape reduced the mean tumor dose by almost a factor of 10 for ^{131}I and 80 for ^{90}Y and increased the activity concentration required to achieve the same theoretical tumor control probability by a factor of 2 for ^{131}I and a factor of 13 for ^{90}Y, as tumor size was reduced from 10 to 0.1 mm.[22] Charged particle escape must be accounted for in predicting patient response based on measured therapeutic indices. In the neuroblastoma model, the minimum activity required to achieve a 50% tumor control probability was achieved at tumor diameters ranging from 1-10 mm diameter.

The downside of non-zero electron ranges is lower radiation absorbed doses in small tumors. The upside is that non-zero electron ranges reduce the effect of activity variations on radiation absorbed dose in large tumors. The maximum (continuous slowing down approximation) ranges of electrons generated by ^{67}Cu, ^{131}I, and ^{90}Y are 2.1, 3.4, and 11.3 mm, respectively, in soft tissue. For all practical gamma emitters, activity distributions can be measured with planar imaging (2D) and Single Photon Emission Computed Tomography (SPECT – 3D). The built-in variations in absorbed dose/activity-response variations that exist due to non-zero electron ranges can be used to estimate image resolution requirements. For example, a resolution of 1-2 mm would provide activity maps consistent with the 2-3 mm maximum ranges for ^{67}Cu and ^{131}I.

The other key issue driving observed dose-response heterogeneity is dose prescription. With the current available therapeutic indices, radionuclide dose prescription (mCi) is based on

avoiding unacceptable normal organ toxicity. Therefore, absorbed radiation dose to the normal, dose-limiting organ should drive how much radioactivity is given to the patient.[24, 25] Figure 4 shows how increasing dose uncertainty decreases the dose at which tumor control begins to be observed but also decreases the maximum possible UTCP. The effect of dose uncertainties on a conventional radiation therapy-derived NTCP curve for kidney complications was calculated by summing tumor control or normal tissue complication probabilities generated over a 2x range at 2.5% dose increments, weighted according to a Gaussian distribution with a standard deviation of 10, 20, and 30% for each dose point. Clearly, a 10% dose uncertainty has a small effect, while a 30% dose uncertainty substantially lowers the slope of the NTCP curve, leading to the significant probability of observing complications at lower doses than would be observed with no dose uncertainty.

Figure 5B shows that an increase in standard deviation of 10, 20, and 30% in absorbed dose to the kidney lowers the maximum uncomplicated tumor control probability (UTCP) by 12, 32, and 47%, respectively. The result is that the best attainable cure rate for this therapy (therapeutic index=3) is reduced by these substantial fractions. In this system, the standard deviation of 31% in absorbed radiation dose to the kidney (described by ref. 24) that would have resulted from prescription using injected activity, would have decreased the best achievable uncomplicated cure probability by 47%.

Figure 5 shows how 10, 20, and 30% dose-prescription uncertainties (standard deviations) degrade the maximum observable uncomplicated tumor control for lymphoma/kidney and carcinoma/kidney examples. The standard deviation of 30% represents the likely uncertainty in absorbed radiation dose to the normal organ in the absence of treatment planning. Standard deviations of ~20-30% would be expected for treatments planned with current imaging and dose calculation technology. With new imaging and dosimetry tools, normal-organ dose uncertainties approaching 10% could be envisioned. For therapeutic indices greater than 1, this would result in maximum uncomplicated tumor control probabilities that are within 15% (therapeutic index greater than 1 for lymphoma, greater than 2.7 for carcinoma).

A practical effect of dose uncertainties is apparent in phase I trials: patients are treated in small groups, increasing the administered dose (mCi or radiation absorbed dose) until the maximum tolerated dose (MTD) is found. Patients who receive a dose to the treatment-limiting organ that is on the high side of the error bar will exhibit complications at lower apparent doses. This results in an estimate of the MTD that is too low, and a treatment that never reaches its potential effectiveness.

Therefore, a major goal in targeted radioisotope therapy should be to establish effective approaches to minimize uncertainties in dose-response, particularly for dose-limiting normal tissues, as the organs that drive (by limiting) dose prescription.

Existing targeted radioisotope data

Up to this point, dose-response data for targeted radioisotope therapy has been only modest and somewhat confusing. Targeted radioisotope studies in mouse tumor models have demonstrated a strong dose-response correlation.[26-28] However, early targeted radioisotope studies in humans showed only a modest relationship between radiation absorbed dose and toxicity or tumor response.[29-32] Most trials so far have been conducted in heterogeneous patient populations with advanced disease. However, results reported by Wong,[33] which used chromosomal translocations, a well-established radiation biodosimeter, to estimate radiation

dose, showed that biological effects increased linearly with absorbed radiation dose in bone marrow, whole body radiation dose, and administered radiation activity for patients with metastatic CEA-producing malignancies given ^{90}Y for targeted radionuclide therapy.

Combining cancer and normal-tissue response data represents a significant opportunity for targeted radionuclide therapy planning.[10] In this paper, we demonstrate some of the mutual impact of treatment planning and biological dose-response, based on data obtained with conventional radiation therapy. The real challenge is to develop and assess these concepts with actual targeted radionuclide therapy data. Accurate, patient-specific dose estimates, as described below, should greatly enhance the reliability of this process.

How Treatment Planning Is Improving

Since the mid-1980's several authors have recognized the need for radiation dosimetry-driven treatment planning systems in radioimmunotherapy.[30, 34-38] Over the past few decades, significant progress has been made in the four areas described below.[39, 40]

Characterizing activity and its distribution

This process involves two levels of sophistication: quantifying the amount of radioactivity administered/decayed/excreted and imaging the 2- or 3-dimensional distribution of activity in the body as a function of time. Obtaining sufficiently accurate quantitative images of activity in the body remains a major challenge in targeted radionuclide dosimetry, due to inadequate correction methods for the effects of radiation attenuation and scatter in both the patient and detector (collimator) system.[41] Another continuing challenge is to model radioactive source kinetics in the body. This has been done using direct integration, least squares analysis, and compartmental modeling.[42]

Characterizing the geometry and composition of the patient

Descriptions of the patient geometry range from mass/surface area to cylinder/ellipsoid "Standard Man" approximation to individualized patient anatomy based on computed tomography (CT) or magnetic resonance imaging (MRI) scans. The underlying anatomical imaging technology has been well developed for other diagnostic purposes, and the primary challenge for targeted radioisotope therapy is to fully utilize the information available. A key part of this process is accurate mapping of radioisotope distribution onto the CT-based anatomy map. Current technology (activity and anatomy scans taken on different machines) result in co-registration errors of 6-10 mm[43, 44] Figure 6 shows how inadequate image co-registration can result in an inaccurate dose distribution for activity concentrated in the liver for a late-stage breast cancer patient. Figure 6A shows co-registered SPECT-CT images that serve as input to a Monte Carlo radiation dose simulation.[†] [45] The high activity in the liver that is partially (and erroneously) registered in the lower-density lung. This results in a substantially higher dose in the lung than would have been observed with a properly registered activity map.

[†] This simulation was done with the PEREGRINE Monte Carlo code system, with energy cutoffs and transport methods described in reference 45.

Estimating the radiation dose in the patient

Several methods have been developed for estimating radiation dose in the patient, ranging from reference tables derived from cylinder/ellipsoid Standard Man model calculations[46-50] to point-kernel approaches [35, 39, 51-54] to direct, stochastic (Monte Carlo) simulation of radiation dose deposition in the patient.[55-57] These models must be combined with methods for describing the time-dependent changes in activity concentration.[58] Direct, stochastic (Monte Carlo) simulation of radiation transport in a CT-based representation the patient provides the most accurate estimate of radiation absorbed dose, reducing 10-25% uncertainties realized with a Standard-Man model to on the order of a few percent.[57] As computer speeds rapidly improve, direct Monte Carlo simulations are becoming increasingly practical. However, the potential of Monte Carlo radiation transport has remained untapped in the context of practical patient trials.

Reporting radiation absorbed dose in tumor(s) and normal organs

The basic output of a treatment planning system consists of time-integrated absorbed dose distributions in the patient's tumor(s) and sensitive normal organs. A set of images may be generated in which intensity represents absorbed dose, or isodose contours or color washes (as shown in Figure 6) may be superimposed on CT images. Dose volume statistics may also be generated. These data provide information regarding the fraction of an organ or tumor that receives a particular absorbed dose or dose range.[59] As more reliable biological-response data for targeted radionuclide therapy becomes available, this information could be combined with tumor control and normal tissue complication probabilities to yield a range of uncomplicated tumor control probabilities, based on the therapeutic indices measured in the patient. Then, the clinician would prescribe the radionuclide dose that maximizes the patient's projected uncomplicated tumor control probability, based on expected variations in therapeutic index due to heterogeneity in tumor size and radionuclide uptake. Figure 7 shows an example of how this more outcome-oriented output might look.

Future Technological Developments

If current imaging and simulations technology is brought to bear, uncertainties in the absorbed radiation dose to normal organs such as the lung, liver, and kidney could be reduced to about 20% (one standard deviation). As shown in Figure 6, this represents a substantial improvement in maximum uncomplicated tumor control compared to the 30% uncertainty likely to be present with radionuclide activity-based prescriptions. However, it still leaves room for improvement, and uncertainties on the order of 10% would clearly bring the maximum uncomplicated tumor control closer to the theoretical limit.

Reducing dosimetric uncertainties to 10% and lower requires careful attention to accuracy in all phases of the treatment planning process. Experience in conventional radiation therapy has shown that accurate (substantially less than 10% uncertainty) radiation absorbed dose estimates can be obtained by combining accurate characterization of the radiation source with a CT scan describing the patient's anatomy with modern radiation transport methods. The challenge for targeted radionuclide therapy is to improve the characterization of radiation sources from planar and SPECT radionuclide images. Ideally, imaging accuracy and spatial resolution would be improved from current levels of 20-30% and 7-15 mm[41] to less than 10% and 1 mm (comparable to electron-density anatomy maps provided by the CT scan).

Current planar or SPECT systems are limited by two key factors: (1) spatial resolution is limited by scattering and absorption of gamma-rays (patient and collimator) and the resolution of the instrument and (2) low count rates can result in relatively high statistical uncertainties for practical three-dimensional imaging. Both of these factors impact on the ultimate accuracy of activity quantification.

Current limitations result from the parallel-hole collimator + scintillator concept. In this system, the collimator defines the direction of the detected gamma rays by selecting out only those that are incident parallel to the collimator holes. The scintillator determines the location and energy of each detected gamma ray. Available parallel-hole collimator / single-crystal scintillator systems reflect the trade-off between efficiency* and resolution (efficiencies ranging from about 10^{-5}-10^{-4} and resolutions ranging from about 5-15 mm) in the context of providing the best possible scatter rejection. Generally, the energy resolution of current scintillation detectors limits efforts to reject scattered gamma rays. Also, collimator-hole size and the light-collection process in single-crystal detectors degrade spatial resolution.

Several approaches are being adapted from basic nuclear physics and astrophysics to provide high spatial resolution, reduce the impact of scatter, and improve detection efficiency. These include new collimator concepts with 1-3 mm spatial resolution[60, 61] and solid-state detectors with improved spatial and energy resolution (less than 3 mm spatial and 2% energy).[62] Also, Positron Emission Tomography (PET), which provides improved quantitation and resolution over conventional SPECT, offers attractive possibilities, provided that a positron-emitting isotope analog is available for the treatment isotope.

Finally, new signal-processing approaches promise to allow one to discard the collimator altogether in favor of a high-resolution detector that determines the gamma-ray direction by gamma-ray tracking.[64, 65] Employing new collimatorless imaging techniques promise to allow a spatial resolution of about 1-2 mm in the patient and a detection efficiency of 10^{-2}-10^{-3}. It may also be possible to accommodate simultaneous CT and activity detection. This means that three-dimensional activity and anatomy can be obtained simultaneously, with the same resolution.

Because of improved resolution, co-registration, and scatter/attenuation corrections, it is likely that the accuracy of this new detection system could approach a quantitative accuracy of 10%. This would effectively eliminate the degrading effect of organ-dose uncertainty shown in Figure 6. The high spatial resolution of detecting tagged molecular targeting agents increases the range of tumors that could be detected, and opens possibilities for substantial more detailed, non-invasive detection of cancer in general.

Impact on Clinical Outcome

Technological innovations in imaging and other aspects of radiation absorbed dose quantification could significantly improve in the accuracy of treatment planning. However, for current and future technology to make an impact, it must be packaged in a form that is easy to integrate into patient care. This is a crucial link that must be reinforced each time new technology becomes available.

Given this integration, a relevant question in the development of targeted radionuclide therapy is how the impact of technological improvements in treatment planning compare with simply improving targeting effectiveness. Figure 4 shows a dramatic rise in maximum

* We define detection efficiency as the number of detected gamma-rays per number of emitted gamma rays.

uncomplicated tumor control probability (UTCP) as the therapeutic index increases. It also suggests that for lung, kidney, and liver, currently-observed therapeutic indices have the potential to result in high probabilities of tumor response. Higher activity concentrations are required to obtain the same therapeutic indices for smaller (unseen) tumors as are measured with observable lesions, due to the effect of charged particle escape. For lower therapeutic indices, relatively small increases in therapeutic index are likely to substantially improve response rates, and could even result in cure, if a sufficient therapeutic index can be maintained in the smallest cancer sites.

However, Figure 5 demonstrates that uncertainties in dose prescription (absorbed dose estimates in the normal, dose-limiting organ) can substantially broaden the UTCP curve and reduce its maximum height. That is, some tumor control will be observed at lower doses, but the potential high probability of tumor control will never be reached. Figure 5 shows how uncertainties in dose prescription degrade the maximum UTCP as a function of therapeutic index, which characterizes drug-targeting effectiveness. Dosimetric uncertainties result in a substantially slower rise in maximum UTCP as the therapeutic index increases. For example, the maximum UTCP associated with therapeutic index of ~5 reported by DeNardo et al.[20] for breast carcinoma would not have been reached until a therapeutic index of about 10 in the presence of the 30% standard deviation associated with mCi/kg prescription methods suggested by Juweid et al.[24] and DeNardo[25].

Conclusions

Results for high-dose myeloablative therapy suggest the possibility of significant tumor control, particularly for lymphoma.[18] In this update, we have put forward the concept of uncomplicated tumor control probability, which is meant to provide an objective assessment of the potential effectiveness of a targeted radionuclide treatment.

Because of the limited radiation dose-response data available for targeted radionuclide therapy, we have used radiation-response data generated from conventional radiation therapy to generate initial estimates to guide our initial assessment of treatment planning needs for this very new form of therapy. The reasonableness of this approach is supported by the consistency in maximum tolerated dose measured for lung in the myeloablative, targeted radionuclide therapy for B-cell lymphoma trial reported by Press et al.[18] and the lung tolerance dose evaluated for conventional radiation therapy by Emami et al.[8] Also, the 84% complete response rate (tumor control for measurable tumors) observed by Press et al. is consistent with the maximum uncomplicated tumor control probability that we predict for the tumor-lung therapeutic index reported.[18]

Uncomplicated tumor control probabilities generated from conventional radiation therapy data suggest that, in a myeloablative regimen, a reasonable probability of uncomplicated tumor control is possible for lymphoma and radiosensitive carcinoma at therapeutic indices that are available now. Relatively small increases in therapeutic index would result in substantial gains in uncomplicated tumor control probability, particularly for carcinoma.

At current therapeutic indices, uncertainty in the assessment of radiation absorbed dose in radiation-sensitive normal organs can make a substantial impact on the uncomplicated tumor control probability. Another important factor is cancer dose-heterogeneity, which results from uneven drug uptake in larger tumors and radioemissions leaving the cancer as they deliver their energy to small tumors.

The goal of a treatment planning system is to provide information that enables the physician to optimize the activity to be delivered and estimate how much the patient will benefit from the treatment. The input to the treatment planning system is 2- and 3-dimensional distributions of activity that change as a function of time, combined with a 3-dimensional map of the patient's anatomy. From this information, a dose-calculation system can estimate the space- and time-dependent radiation dose distribution in the patient. We argue that the ideal treatment planning system would combine this physical information with biological radiation-response data to predict the ideal dose to be administered and estimate uncomplicated tumor control probabilities for the range of tumor sizes expected in the patient.

Current imaging and radiation simulations technology supports treatment planning uncertainties (1 standard deviation) of about 20%, with 7-15 mm-resolution radionuclide activity distributions being a major limitation. However, new developments in gamma-ray imaging, including new detector technologies and the expanded use of PET, promise substantially smaller uncertainties of around 1-2 mm (resolution and co-registration) and ~10% (activity quantitation). Treatment planning systems based on new imaging methods, combined with accurate radiation dose simulations, promise to meet and exceed the resolution, co-registration, and dose-accuracy requirements, making accurate, efficient treatment planning likely to be an important component of targeted radionuclide delivery for the future.

References

1. Perez CA, Brady LW ed. *Principals and Practice of Radiation Oncology. Third Edition,* Lippincott-Raven Publishers, Philadelphia, PA. 1998.
2. DeNardo SJ, Kroger LA, DeNardo GL. A new era for radiolabeled antibodies in cancer? *Current Opinion in Immunology* 1999; 11:563-569.
3. Meischner G. Erfolge der karzinombehandlung an der Dermatologischen Klinik Zurich. Einzeitige Hochstosis and Fraktionierte Behandlung. *Strahlungtherapie* 1934; 49:65-81.
4. Strandqvist M. Studien uber diekumulative wirkung der roentgenstrahlen bie frakionierung. *Acta Radiol Suppl (Stockh)* 1944; 55:1-300.
5. Shukovsky LJ. Dose, time, volume relationships in squamous cell carcinoma of the supraglottic larynx. *Am J Roentgenol* 1970; 108:27-29.
6. Fletcher GH. Clinical dose-response curve of human malignant epithelial tumors. *Br J Radiol* 1973; 46:1-12.
7. Meoz-Mendez RT, Fletcher GH, Guillamondegui OM ,et al. Analysis of the results of irradiation in the treatment of squamous cell carcinomas of the pharyngeal walls. *Int J Radiat Oncol Biol Phys* 1983; 4:579-585.
8. Emami B, Lyman J, Brown A, Coia L, Goitein M, Munzenrider JE, Shank B, Solin LJ, Wesson M. Tolerance of normal tissue to therapeutic radiation. *Int J Radiat Oncol Biol Phys* 1991; 21:102-122.
9. Brahme A. Dosimetric precision requirements in radiation therapy. *Acta Radiol Oncol* 1985; 23: 379-391.
10. DeNardo SJ, Williams LE, Leigh BR, Wahl R. Radioimmunotherapy: Choosing an optimal dose for clinical response. *Cancer* accepted for pubication 2002.
11. Sgouros G. Treatment planning for internal emitter therapy: methods, applications and clinical implications. notes from lecture at June, 2000 Society of Nuclear Medicine.
12. Fischer DB, Fischer JJ. Dose response relationships in radiation therapy. Application of the logistic regression model. *Int J Radiat Oncol Biol Phys* 1977; 2 773.
13. Niemierko A, Goitein M. Calculation of normal tissue complication probability and dose-volume histogram reduction schemes for tissues with a critical element architecture. *Radiotherapy and Oncology* 1991;166-176.
14. Agren CA, Lallman P, Turesson I, et al. Volume and heterogeneity dependence of the dose-response relationship for head and neck tumours. *Acta Oncol* 1995;34:851.
15. Burman C, Kutcher GJ, Emami B, Goitein M. Fitting of normal tissue tolerance data to an analytic function. *Int J Radiat Oncol Biol Phys* 1991;21:123-135.
16. Fletcher GH, Shukovsky LJ. The interplay of radiocurability and tolerance in the irradiation of human cancers. *J Radiol Electrol Med Nucl* 1975;56(5):383-400.
17. Mendelsohn ML. The biology of dose-limiting tissues. in Time and Dose Relationships in Radiation Biology as Applied to radiotherapy, Brookhaven National Laboratory (BNL) Report 5023 (C-57);1969; pp 154-173. Upton, NY, Brookhaven National Laboratory.

18. Press OW, Eary JF, Appelbaum FD, Martin PJ, Nelp WB, Glenn S, Fisher DR, Porter B, Matthews DC, Gooley T, Bernstin ID. Phase II trial of ^{131}I (anti-CD20) antibody therapy with autologous stem cell transplantation for relapsed B cell lymphomas. *Lancet* 1995;346:336-340.

19. DeNardo GL, DeNardo SJ, O'Donnell RT, Kroger LA, Kukis DL, Meares CF, Goldstein DS, Shen S. Are radiometal-labeled antibodies better than 131I-labeled antibodies: comparative pharmacokinetics and dosimetry of copper-67-, iodine-131-, and yttrium-90-labeled Lym-1 antibody in patients with non-Hogkin's lymphoma. *Clinical Lymphoma*;2000;1:118.

20. DeNardo SJ, Richman CM, Goldstein DS, Shen S, Salako QA, Kukis DL, Meares CF, Yuan A, Welborn JL, DeNardo GL. Yttrium-90/indium-111-DOTA-peptide-chimeric L6: pharmacokinetics, dosimetry and initial results in patients with incurable breast cancer. *Anticancer Res* 17: 1997;1735-1744.

21. Wheldon TE, O'Donoghue JA, Barrett A, Michalowski A S. The curability of tumors of different size by targeted radiotherapy using ^{131}I or ^{90}Y. *Radiother. Oncol*. 1991;21 91-99.

22. Nahum AE. Microdosimetry and radiocurability: modeling targeted therapy with _-emitters. *Phys Med Biol* 1996;41 1957-1972.

23. DeNardo DA, DeNardo GL, Yuan A, Shen S, DeNardo SJ, Macey DJ, Lamborn KR, Mahe MA, Groch MW, Erwin WD. Prediction of radiation doses from therapy using tracer studies with Iodine-131 labeled antibodies. *J Nucl Med* 1996;37:1970.

24. Juweid ME, Hajjar G, Stein R et al. Initial experience with high-dose radioimmunotherapy of metastatic medullary thyroid carcinoma using ^{131}I-MN-14 F(ab)$_2$ anti-carcinoembryonic antigen monoclonal antibody and autologous hematopoietic stem cell rescue. *J Nucl Med* 2000;41:93-103.

25. DeNardo SJ. Tumor-targeted radionuclide therapy: Trial design driven by patient dosimetry. *J Nucl Med* 2000;41:1 104-106.

26. DeNardo GL, Kukis DL, Shen S, Mausner LF, Meares CF, Srivastava SC, Miers LA, DeNardo SJ. Efficacy and toxicity of ^{67}Cu-2IT-BAT-Lym-1 radioimmunoconjugate in mice implanted with Burkitt's lymphoma (Raji). *Clin Cancer Res* 1997;3:71-79.

27. DeNardo GL, Kroger LA, Denardo SJ, Miers LA, Salako Q, Kukis DL, Fand I, Shen S, Renn O, Mears CF. Comparative toxicity studies of yttrium-90 MX-DTPA and 2-IT-BAD conjugated monoclonal antibody (BrE-3). *Cancer* 1994;73: 1012-1022.

28. Buchsbaum DJ, Wahl RL, Glenn SD, Normolle DP, Kaminski MS. Improved delivery of radiolabeled anti-B1 monoclonal antibody to Raji lymphoma xenografts by predosing with unlabeled anti-B1 monoclonal antibody. *Cancer Res* 1992;52:637-642.

29. Goldenberg DM, Horowitz JA, Sharkey RM, Hall TC, Murthy S, Goldenberg H, Lee RE, Stein R, Siegel JA, Izon DO, Burger K, Swayne LC, Belisle E, Hansen HJ, Pinske CM. Targeting, dosimetry, and radioimmunotherapy of B-cell lymphomas with iodine-131-labeled LL2 monoclonal antibody. *J Clin Oncol* 1991;9:548-564.

30. Juweid ME, Zhang CH, Blumenthal RD, et al. Factors influencing hematologic toxicity of radioimmunotherapy with 131I-labeled anti-carcinoembryonic antigen antibodies. *Cancer* 1997;80:2749-2753.

31. Lamborn KR, DeNardo GL, Denardo SJ, Goldstein DS, Shen S, Larkin EC, Kroger LA. Treatment-related parameters predicting efficacy of Lym-1 radioimmunotherapy in patients with B-lymphocytic malignancies. *Clin Cancer Res* 1997;3:1253-1260.

32. Vriesendorp HM, Quadri SM, Andersson BS, Dicke KA. Hematologic side effects of radiolabeled immunoglobulin therapy. *Exp Hematol* 1996;24:1183-1190.

33. Wong JY, Wang J, Liu A, Odom-Maryon T, Shively JE, Raubitschek AA, Williams LE. Evaluating changes in stable chromosomal translocation frequency in patients receiving radioimmunotherapy. *Int J Radiation Oncol Biol Phys* 2000;46:599-607.

34. DeNardo GL, Raventos A, Hines HH, et al. Requirements for a treatment planning system for radioimmunotherapy. *Int J Radiat Oncol Biol Phys* 1985;11:335-348.

35. Sgouros G, Barest G, Thekkumthala J, et al. Treatment planning for internal radiation therapy: Three-dimensional dosimetry for nonuniformly distributed radionuclides. *J Nucl Med* 1990;31:1884—1891.

36. Tagesson M, Ljungberg M, Strand SE. Monte Carlo program converting activity distributions to absorbed dose distributions in a radionuclide treatment planning system. *Acta Oncol* 1996;35: 367-372.

37. Williams LE. Estimation of absorbed doses in radioimmunotherapy. *Med Phys* 1995;22:958.

38. Johnson TK. MABDOS: A generalized program for internal radionuclide dosimetry. *Computer Methods Programs Biomed* 1988;27:159-167.

39. Erdi AK, Erdi YE, Yorke ED, Wessels BW. Treatment planning for radioimmunotherapy. *Phys Med Biol* 1996;41:2009-2026.

40. Zanzonico P B. Internal radionuclide radiation dosimetry: A review of basic concepts and recent developments. *J Nucl Med* 2000;41(2) 297-308.

41. Strand S-E, Jönsson B-A, Ljungberg M, Tennvall J. Radioimmunotherapy dosimetry – A review. *Acta Oncologica* 1993;32(7-8): 807-817.

42. Stabin MG. MIRDOSE: personal computer software for internal dose assessment in nuclear medicine. *J Nucl Med* 1996;37:538-546.

43. Erdi YE, Wessels BW, DeJager R, Erdi AK, Der L, Cheek Y, Shiri R, Yorke E, Altemus R, Varma V, Smith LE, Hanna MG. A new fiducial alignment system to overlay abdominal computed tomography or magnetic resonance anatomical image with radiolabeled antibody single-photon emission computed tomographic scans. *Cancer* (Suppl) 1994;73(3):923-931.

44. Scott AM, Macapinlac HA, Divgi CR, Zhang JJ, Kalaigian H, Pentlow K, Hilton S, Graham MC, Sgouros G, Pelizzari C, Chen G, Schlom J, Goldsmith SJ, Larson SM. Clinical validation of SPECT and CT/MRI image registration in radiolabeled monoclonal antibody studies of colorectal carcinoma. *J Nucl Med* 1994;35(12):1976-1984.

45. C. L. Hartmann Siantar, R. S. Walling, T. P. Daly, B. Faddegon, N. Albright, Paul Bergstrom, A. F. Bielajew, C. Chuang, D. Garrett, R.K. House, D. Knapp, D. J. Wieczorek, L. J. Verhey. Description and dosimetric verification of the PEREGRINE Monte Carlo dose calculation system for photon beams incident on a water phantom. *Med Phys* 2001;28(7) 1322-1337.

46. Snyder WS, Ford MR, Warner GG. Estimates of specific absorbed fractions for photon sources uniformly distributed in various organs of a heterogeneous phantom. MIRD Pamphlet No. 5, Revised. New York: Society of Nuclear Medicine 1978.

47. Howell RW, Wessels BW, Loevinger R, et al. The MIRD perspective 1999. *J Nucl Med* 1999;40:3S-10S.

48. Loevinger R, Berman M. A revised schema for calculating the absorbed dose from biologically distributed radionuclides. MIRD Pamphlet No. 1, Revised. New York: Society of Nuclear Medicine (1976).

49. Stabin MG. MIRDOSE: personal computer software for internal dose assessment in nuclear medicine. *J Nucl Med* 1996;37:538-546.

50. Sgouros G, Bigler R, Zanzonico P. DOSCAL: a tumor-incorporating mean absorbed dose calculation program. *J Nucl Med* 1988;29(Suppl.):874.

51. Sgouros G, Chiu S, Pentlow KS, Brewster LJ, Kalaigian H, Baldwin B, Daghighian F, Graham MC, Larson SM, Mohan R. Three-dimensional dosimetry for radioimmunotherapy treatment planning. *J Nucl Med* 1993;34:1595-1601.

52. Erdi AK, Wessels BW, DeJager R et al. Tumor activity confirmation and isodose curve display for patients receiving iodine-131-labeled 16.88 human monoclonal antibody. *Cancer* 1994;73:932-944.

53. Erdi AK, York ED, Loew MH, Erdi YE, Sarfaraz M, Wessels BW. Use of the fast Hartley transform for three-dimensional dose calculation in radionuclide therapy. *Med Phys* 1998;25:2226-2233.

54. Giap HB, Macey DJ, Bayouth JE, Boyer AL. Validation of a dose-point kernel convolution technique for internal dosimetry. *Phys Med Biol* 1995;40:365-381.

55. Johnson TK, Vessella RL. On the possibility of 'real-time' Monte Carlo calculations for the estimation of absorbed dose in radioimmunotherapy. *Computer Methods Programs Biomed* 1989;29:205-210.

56. Furhang EE, Chiu CS, Sgouros G. A Monte Carlo approach to patient-specific dosimetry. *Med Phys* 1996;23:1523-1529.

57. Furhang EE, Chui CS, Kolbert KS, Larson SM, Sgouros G. Implementation of a Monte Carlo dosimetry method for patient-specific internal emitter therapy. *Med Phys* 1997;24:1163-1172.

58. Stabin MG. Internal dosimetry in the use of radiopharmaceuticals in therapy – Science at a crossroads? *Cancer Biother Radiopharm* 1999;14:81-89.

59. Kolbert KS, Sgouros G, Scott AM, Baldwin B, Zhang J, Kalaigian H, Macapinlac HA, Graham MC, Larson SM. Dose-volume histogram representation of patient dose distribution in three-dimensional internal dosimetry. *J Nucl Med* 1994;35: 123P.

60. MacDonald LR, Patt BE, Iwanczyk JS, Tsui BMW, Wang Y, Frey EC, Wessell DE, Acton PD, Kung HF. Pinhole SPECT of mice using the LumaGEM gamma camera. *IEEE Trans Nucl Sci* 2001;48(3): 830-836.

61. Durrant PT, Dallimore M, Jupp ID, Ramsden D. The application of pinhole and coded aperture imaging in the nuclear environment. *Nuclear Instruments and Methods in Physics Research* 1999;A422: 667-671

62. Rogulski MM, Barber HB, Barrett HH, Shoemaker RL, Woolfenden JM. Ultra-high resolution brain SPECT imaging: simulation results. *IEEE Trans. Nucl. Sci*. 40(4): 1123-1129.

63. Vetter K, Kuhn, A, Deleplanque MA, Lee IY, Stephens FS, Schmid GJ, Beckedahl DA, Blair JJ, Clark RM, Cromaz M, Diamond RM, Fallon P, Lane GJ, Kammeraad JE, Macchiavelli AO, Svensson CE. Three-dimensional position sensitivity in two-dimensionally segmented HP-Ge detectors. *Nuclear Instruments and Methods in Physics Research* 2000;A452: 223-238.

64. LeBlanc JW, Clinthorne NH, Hua C, Rogers WL, Wehe DK, Wilderman SJ. A Compton camera for nuclear medicine applications using ^{113m}In. *Nuclear Instruments and Methods in Physics Research* 1999;A422: 735-739.

65. Smith LE, Chen C, Wehe DK, He Z. Hybrid collimation for industrial gamma-ray imaging: combining spatially coded and Compton aperture data. *Nuclear Instruments and Methods in Physics Research* 2001;A462: 576-587.

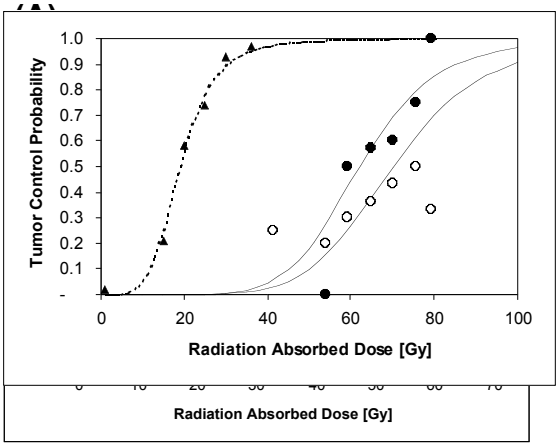

Figure 1. Relationship between tumor control or normal tissue complication probability and radiation absorbed dose for representative tumor and normal tissues. (A) shows representative tumor control probability (TCP) for Hodgkin's lymphoma[16] (_) and carcinoma of the nasopharynx[14] (o for T1-2 and _ for T3-4) (B) shows representative normal tissue complication probability (NTCP) for the three most radiosensitive critical organs for a myeloablative therapy: the lungs (_), kidneys (o), and liver (_). Complication endpoints are pneumonitis, clinical nephritis, and liver failure. The liver and kidneys are about a factor of two more sensitive than tumor. Also, the dose-dependent onset of effects is significantly steeper for the normal tissues than for tumor. This is probably due to the greater conformity in dose-response for normal tissues than for tumor.

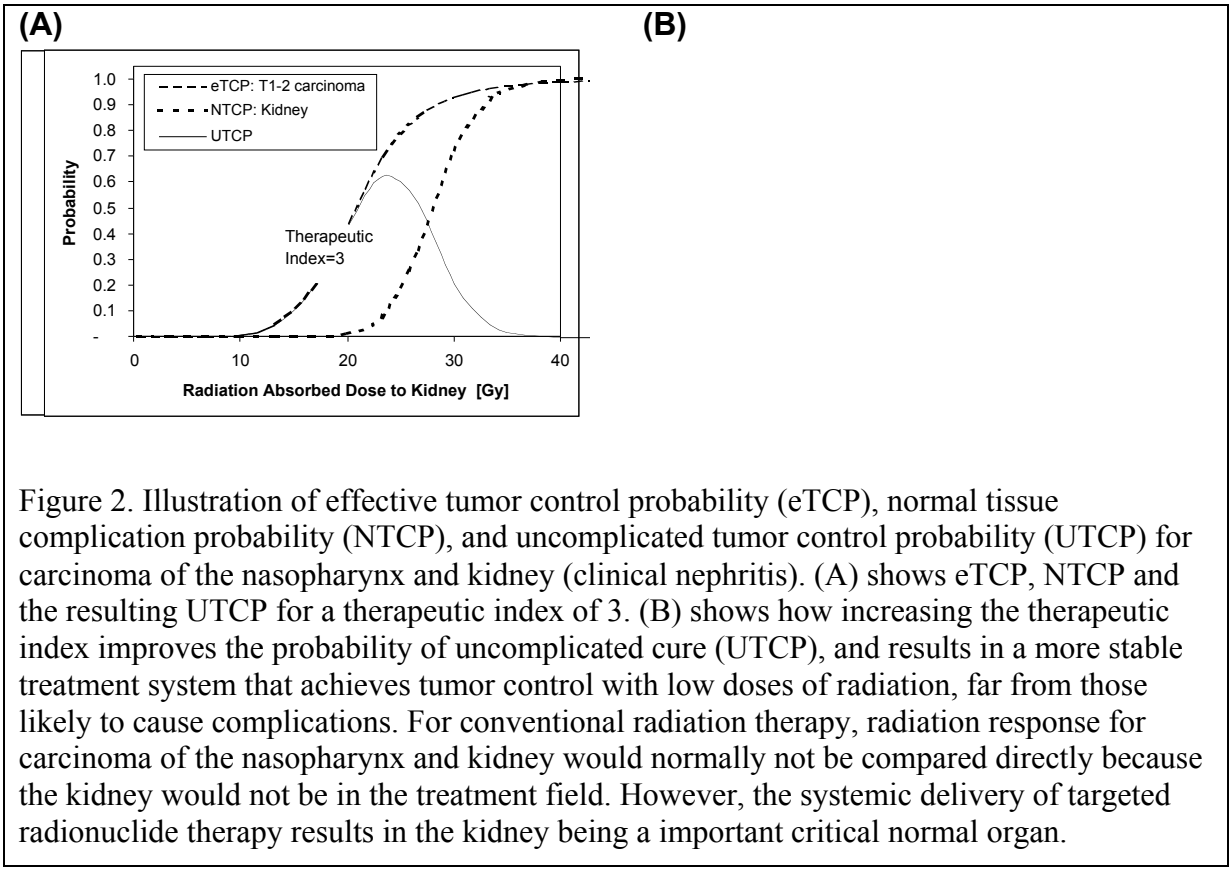

Figure 2. Illustration of effective tumor control probability (eTCP), normal tissue complication probability (NTCP), and uncomplicated tumor control probability (UTCP) for carcinoma of the nasopharynx and kidney (clinical nephritis). (A) shows eTCP, NTCP and the resulting UTCP for a therapeutic index of 3. (B) shows how increasing the therapeutic index improves the probability of uncomplicated cure (UTCP), and results in a more stable treatment system that achieves tumor control with low doses of radiation, far from those likely to cause complications. For conventional radiation therapy, radiation response for carcinoma of the nasopharynx and kidney would normally not be compared directly because the kidney would not be in the treatment field. However, the systemic delivery of targeted radionuclide therapy results in the kidney being a important critical normal organ.

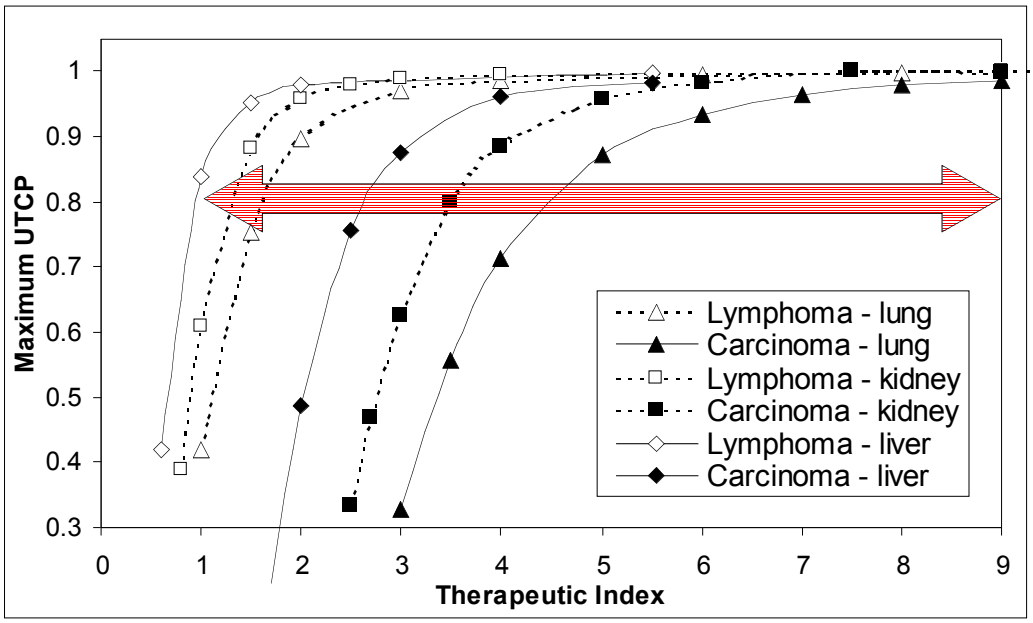

Figure 3. Maximum uncomplicated tumor control probability as a function of therapeutic index for lung (triangle), kidney (square), and liver (diamond) with lymphoma (dashed line) and carcinoma (full line). The red arrow shows the range of therapeutic indices observed be DeNardo et al. for lung and kidney in their Lym-1/lymphoma system. This represents only the maximum possible uncomplicated tumor control, in a perfect system. Actual tumor control would depend on the amount of radioactive drug administered. The uncomplicated tumor control profile observed in a trial could also depend strongly on the uncertainty in dose to normal tissues, as shown in Figure 5.

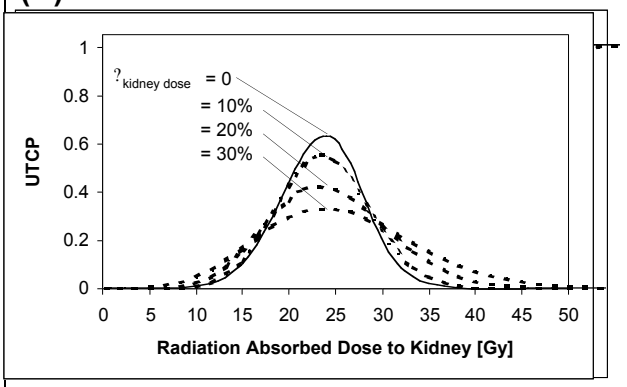

Figure 4. Effect of radiation absorbed dose uncertainty in the kidney, $\_D_{kidney}$, in terms of normal tissue complications (NTCP), tumor control probabilities (eTCP), and uncomplicated tumor control probabilities (UTCP) for carcinoma of the nasopharynx, assuming a fixed therapeutic index of 3. (A) shows the effect of a 20% standard deviation in kidney dose on the eTCP and $NTCP_{kidney}$. (B) shows the effect of 10, 20, and 30% standard deviations in kidney dose on the UTCP.

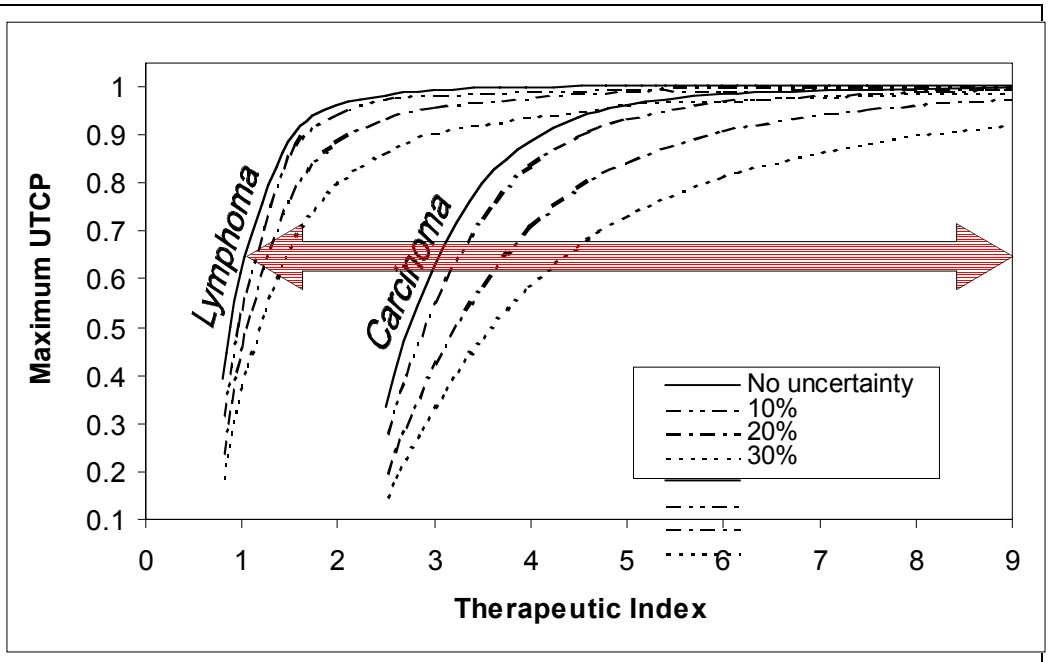

Figure 5. Graphical comparison of how a 10%, 20%, and 30% uncertainty in the radiation absorbed dose to the dose-limiting organ reduces the maximum observed uncomplicated tumor control probability (UTCP) for the lymphoma/carcinoma and kidney (clinical nephritis). The red shaded arrow represents the range of therapeutic indices reported by Denardo et al.[19] in the lungs, kidneys, and liver, with a tumor control probability consistent with carcinoma.

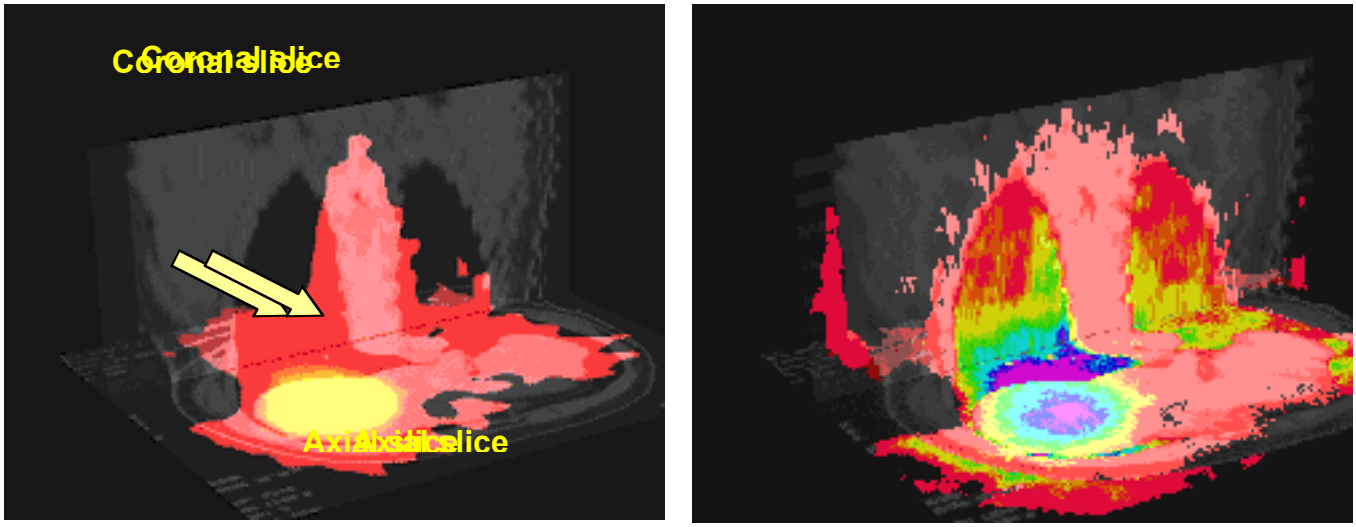

Figure 6. Coronal- and axial-slice views of a fused CT/SPECT image (A) and CT/radiation absorbed dose images (B), shown as a color wash for a patient with advanced breast cancer. For (A), high-low activity is shown by yellow-red-no color. In (B), high-low activity is shown as purple-blue-aqua-green-yellow-red-clear. The high activity in the liver is partially registered in the lower-density lung (see arrow). This result in an erroneously high radiation absorbed dose predicted in the lung, and insufficient activity in the liver. This problem arises because the patient was scanned on different days and different positions: the SPECT was obtained with arms down, while the CT was obtained with arms up.

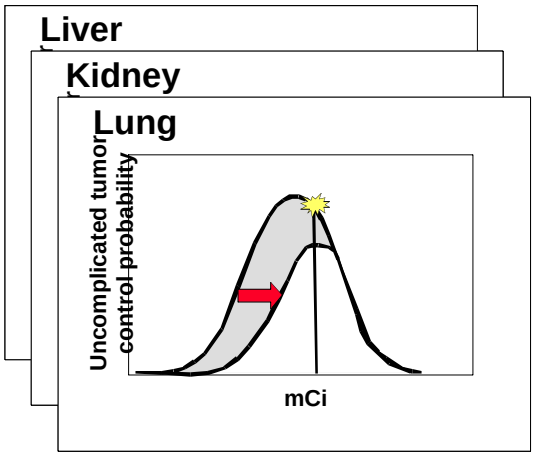

Figure 7. Ideal output of an outcome-oriented treatment planning system. Based on therapeutic indices measured for the patient's tumor(s) and potential dose-limiting organs, the system would calculate a range of projected uncomplicated tumor control probability (UTCP) curves. Then, the clinician would prescribe the radionuclide dose that optimizes the UTCPs for the cancer and critical organs.